

RESEARCH ARTICLE

Revealing the novel metabolism-related genes in the ossification of the ligamentum flavum based on whole transcriptomic data

Yongzhao Zhao^{1,2,3} | Qian Xiang^{1,2,3} | Shuai Jiang^{1,2,3} | Jialiang Lin^{1,2,3} | Weishi Li^{1,2,3}

¹Department of Orthopaedics, Peking University Third Hospital, Beijing, China

²Beijing Key Laboratory of Spinal Disease Research, Beijing, China

³Engineering Research Center of Bone and Joint Precision Medicine, Ministry of Education, Beijing, China

Correspondence

Weishi Li, Department of Orthopedics, Peking University Third Hospital, Beijing Key Laboratory of Spinal Disease Research, Engineering Research Center of Bone and Joint Precision Medicine, Ministry of Education, Peking University, No. 49 North Garden Road, Haidian District, Beijing, 100191, China.
Email: puh3liweishi@bjmu.edu.cn

Funding information

National Natural Science Foundation of China, Grant/Award Number: 82172480

Abstract

Backgrounds: The ossification of the ligamentum flavum (OLF) is one of the major causes of thoracic myelopathy. Previous studies indicated there might be a potential link between metabolic disorder and pathogenesis of OLF. The aim of this study was to determine the potential role of metabolic disorder in the pathogenesis of OLF using the strict bioinformatic workflow for metabolism-related genes and experimental validation.

Methods: A series of bioinformatic approaches based on metabolism-related genes were conducted to compare the metabolism score between OLF tissues and normal ligamentum flavum (LF) tissues using the single sample gene set enrichment analysis. The OLF-related and metabolism-related differentially expressed genes (OMDEGs) were screened out, and the biological functions of OMDEGs were explored, including the Gene Ontology enrichment analysis, Kyoto Encyclopedia of Genes and Genomes enrichment analysis, and protein–protein interaction. The competing endogenous RNA (ceRNA) network based on pairs of miRNA-hub OMDEGs was constructed. The correlation analysis was conducted to explore the potential relationship between metabolic disorder and immunity abnormality in OLF. In the end, the cell experiments were performed to validate the roles of GBE1 and TNF- α in the osteogenic differentiation of LF cells.

Results: There was a significant difference of metabolism score between OLF tissues and normal LF tissues. Forty-nine OMDEGs were screened out and their biological

Abbreviations: ALP, alkaline phosphatase; ARS, Alizarin Red S; ceRNA, competing endogenous RNA; circRNA, circular RNA; DEGs, differentially expressed genes; DEmiRNAs, differentially expressed miRNAs; GO, gene ontology; KEGG, Kyoto Encyclopedia of Genes and Genomes; LF, ligamentum flavum; lncRNA, long non-coding RNA; miRNA, microRNA; MSC, mesenchymal stem cell; OIICs, OLF-related infiltrating immune cells; OLF, ossification of the ligamentum flavum; OMDEGs, OLF-related and metabolism-related differentially expressed genes; PCA, principal component analysis; PPI, protein–protein interaction; ssGSEA, single sample gene set enrichment analysis.

Yongzhao Zhao, Qian Xiang, Shuai Jiang contributed equally to this work.

This is an open access article under the terms of the [Creative Commons Attribution-NonCommercial-NoDerivs](https://creativecommons.org/licenses/by-nc-nd/4.0/) License, which permits use and distribution in any medium, provided the original work is properly cited, the use is non-commercial and no modifications or adaptations are made.

© 2024 The Author(s). *JOR Spine* published by Wiley Periodicals LLC on behalf of Orthopaedic Research Society.

functions were determined. The ceRNA network containing three hub OMDEGs and five differentially expressed miRNAs (DEmiRNAs) was built. The correlation analysis between hub OMDEGs and OLF-related infiltrating immune cells indicated that metabolic disorder might contribute to the OLF via altering the local immune status of LF tissues. The cell experiments determined the important roles of GBE1 expression and TNF- α in the osteogenic differentiation of LF cells.

Conclusions: This research, for the first time, preliminarily illustrated the vital role of metabolic disorder in the pathogenesis of OLF using strict bioinformatic algorithms and experimental validation for metabolism-related genes, which could provide new insights for investigating disease mechanism and screening effective therapeutic targets of OLF in the future.

KEYWORDS

bioinformatic analysis, ceRNA network, experimental validation, immunity abnormality, metabolic disorder, ossification of the ligamentum flavum

1 | INTRODUCTION

Ossification of the ligamentum flavum (OLF), one characteristic disease of ectopic ossification, has become the major cause of thoracic myelopathy.¹ The incidence of OLF varied from 4 to 64%, and most of cases lived in East Asian region, such as Japan, China, and South Korea.¹⁻³ Surgical decompression remains the mainstream treatment for the thoracic myelopathy caused by OLF because OLF is insidious at early phase, however, the thoracic canal decompression is a very complicated operation with high risks of perioperative complications.^{4,5} Moreover, the potential pathogenic factors still exist after the surgery, which may cause the re-ossification of residual ligamentum flavum (LF).⁶ Therefore, it is urgent to fully understand the pathogenesis of OLF to better manage this relatively rare disease.

OLF is a complex and multifactor disease, and several genetic and environmental factors are involved in the disease susceptibility, including genetic genes,⁷ inflammation,⁸ mechanical stress,⁹ and metabolic disorder.¹⁰ Metabolic disorder could lead to or aggravate multiple human diseases, such as cancers,¹¹ diabetes,¹² and immunological diseases.¹³ Previous studies have reported that metabolic disorder might be significantly associated with the onset and progression of OLF.¹⁴⁻¹⁹ Endo et al. study showed there was a distinct association between the severity of thoracic OLF and degree of obesity, and OLF patients had a higher incidence of diabetes compared with non-OLF patients ($p < 0.05$).¹⁴ Similarly, Kim et al. also observed a higher incidence of diabetes in OLF patients compared with non-OLF patients ($p < 0.05$).¹⁸ Besides, the leptin, one kind of adipocytokine secreted by adipose tissues, has been proved to promote the OLF via the regulation of STAT3, Runx2, and SRC-1.^{10,20} In our previous study, we discovered that high body mass index might contribute to the onset and severity of the OLF.^{21,22} Therefore, accumulating evidence showed that metabolic disorder might play a vital role in the pathogenesis of OLF. However, the value of metabolic disorder in OLF has not obtained adequate attention, and underlying mechanism remains unclear to date.

Long non-coding RNAs (lncRNAs) refer to the noncoding RNAs with a length of more than 200 nucleotides and without the protein-coding capacity.²³ Circular RNAs (circRNAs) are the closed back-splicing products of precursor mRNA in eukaryotes, which have the special structure and stable expression.^{24,25} MicroRNAs (miRNAs) are a type of small non-coding RNA with 19–25 nucleotides, which can negatively regulate the gene expression at the posttranscriptional level.²⁶ Plenty of circRNAs or lncRNAs have been proved to perform their diverse biological functions via the competing endogenous RNA (ceRNA) network of circRNA/lncRNA-miRNA-mRNA axis, and dysregulated ceRNA networks have been demonstrated to play important roles in several human diseases.^{25,27,28} But the roles of ceRNA network in the regulation of metabolism-related genes in OLF have not been fully investigated.

Immunity abnormality has been reported to associate with the pathogenesis of OLF. we previously reported that high systemic immune-inflammation index was an independent risk factor of OLF.²² Wang et al. found that serum TNF- α of patients with OLF was significantly higher than those without OLF, and TNF- α significantly promoted the osteogenic differentiation of LF cells.²⁹ Qu et al. reported that M1 macrophage-derived interleukin-6 could facilitate the osteogenic differentiation of LF cells.³⁰ Zhang et al. analyzed the immune cell infiltration landscape, and constructed an immunoregulatory network between the immunocytes and immune-related genes in OLF.³¹ However, the relationship between metabolic disorder and immunity abnormality in OLF has not been investigated to date.

With the advancement of chip sequencing and next generation sequencing technologies, many OLF-related mRNAs and miRNAs have been identified,³² which significantly promote the development of OLF research. A previous bioinformatic analysis was conducted to investigate the role of immunity abnormality in the development of OLF using the sequencing data.³¹ However, metabolic disorder, as another important contributor to OLF, has not been investigated using bioinformatic approaches up to now.

In our study, to further determine the potential role of metabolic disorder in the pathogenesis of OLF, multiple bioinformatic algorithms were conducted to compare the difference of metabolism score between OLF tissues and normal LF tissues, identify hub OLF-related and metabolism-related differentially expressed genes (OMDEGs), illustrate the biological functions, construct the ceRNA network, explore the potential link between metabolic disorder and immunity abnormality in OLF, and validate the findings using further cell experiments.

2 | MATERIALS AND METHODS

This study has been approved by the Ethics Committee of our hospital (PUTH-REC-SOP-06-3.0-A27, #2014003). The written informed consent was obtained in all included patients. The flowchart of this study was showed in Figure 1.

2.1 | Data collection and processing

The miRNA and mRNA data were downloaded from gene expression omnibus database for the differential expression analysis. Two

datasets (GSE106253 and GSE106256) containing 4 thoracic OLF patients and 4 spinal trauma patients were downloaded for further analysis. The GSE106253 contained the mRNA expression profile, and was downloaded based on the platform of GPL21827 (Agilent-079487 Arraystar Human LncRNA microarray V4). The GSE106256 contained the miRNA expression profile, and was downloaded based on the platform of GPL18573 Illumina NextSeq 500 (Homo sapiens). A total of 1383 metabolism-related genes were obtained from three main metabolism pathways (REACTOME METABOLISM OF AMINO ACIDS AND DERIVATIVES, REACTOME METABOLISM OF LIPIDS, and REACTOME METABOLISM OF CARBOHYDRATES) in the Molecular Signatures Database (www.gsea-msigdb.org) (Table S1).

2.2 | Determination of metabolism

To determine whether metabolic disorder was involved in the pathogenesis of OLF, a metabolism score was calculated using the metabolism-related gene list by the single sample gene set enrichment analysis (ssGSEA).³³ Moreover, principal component analysis (PCA) was performed to determine whether there was a difference in the

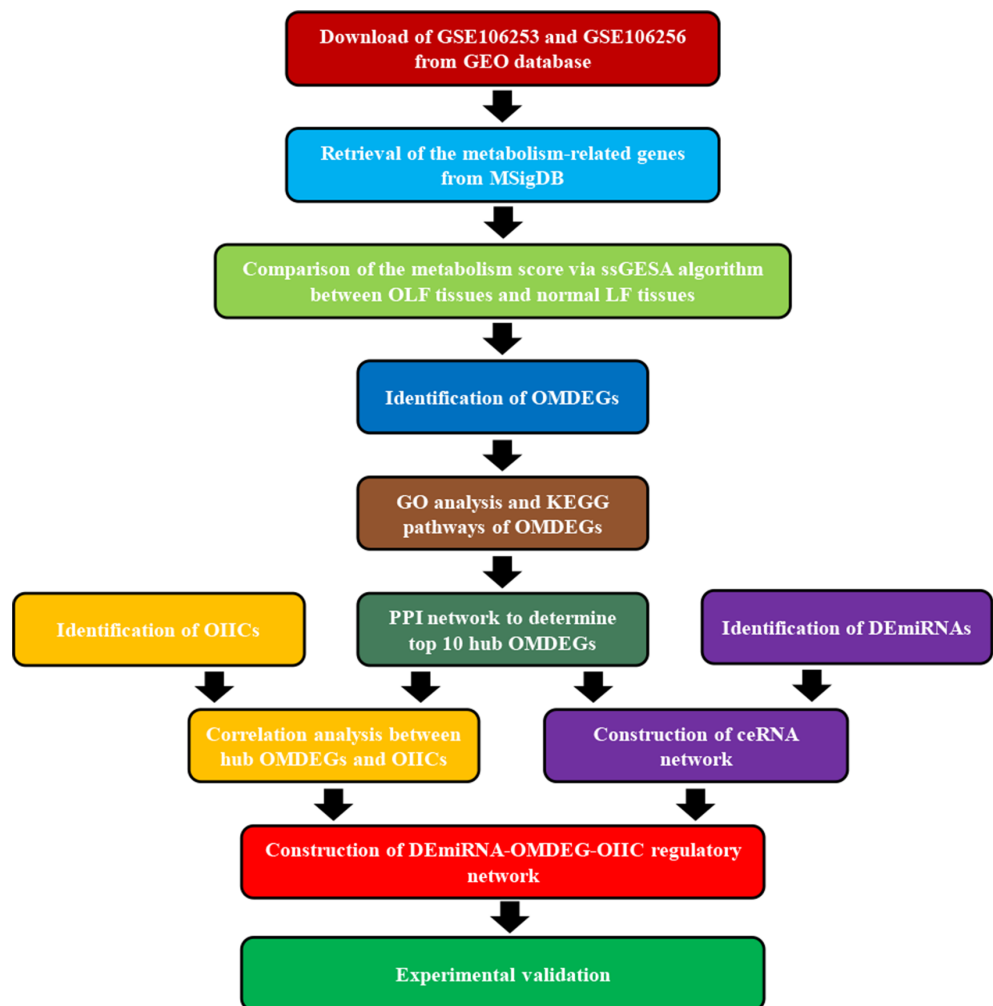


FIGURE 1 Flow chart of bioinformatic algorithms.

metabolism between OLF tissues and normal LF tissues by evaluating the expression of metabolism-related genes.

2.3 | Identification of OMDEGs and differentially expressed miRNAs (DEmiRNAs)

OLF-related differentially expressed genes (DEGs) were obtained using the R package limma package, with the criterion of adjust $p < 0.05$ and fold change > 2 . The OMDEGs were obtained with the intersection of OLF-related DEGs and metabolism-related genes using the Venn diagram. Similarly, DEmiRNAs were obtained using the R package limma package with the criterion of $p < 0.05$ and fold change > 2 .

2.4 | Functional enrichment analysis of OMDEGs

Gene ontology (GO) enrichment analysis and Kyoto Encyclopedia of Genes and Genomes (KEGG) enrichment analysis were performed to explore the potential functions and related signaling pathways of OMDEGs using the DAVID database (<https://david.ncicrf.gov/>). The GO and KEGG pathway terms with $p < 0.05$ were selected for subsequent visualization using the clusterProfiler package in R software.

2.5 | Protein-protein interaction (PPI) network of OMDEGs

The STRING database (<https://string-db.org>) was used to construct the PPI network.¹ The OMDEGs were mapped to STRING list to perform multiple proteins search and get a PPI network with interaction scores > 0.40 . Cytoscape software (V.3.9.0) (<https://cytoscape.org/>) was used to visualize the results from the PPI network, and cytoHubba plug-in was used to determine the top 10 hub OMDEGs ranked by the Degree score.³⁴ The correlation analysis among 10 hub OMDEGs was performed by Pearson test.

2.6 | ceRNA network of lncRNA/circRNA-DEmiRNA-OMDEG axis

The miRNAs targeting the 10 hub OMDEGs were predicted by TargetScan 7.2 (http://www.targetscan.org/vert_72/),³⁵ and then were taken in to the intersection with DEmiRNAs to obtain the candidate DEmiRNAs. The most important biological function of miRNAs is to promote the degradation of mRNAs by binding to the complementary sequences in the 3'-untranslated region of target genes.³⁶ Therefore, the correlation analysis between candidate DEmiRNAs and 10 hub OMDEGs was conducted, and significant DEmiRNA-OMDEG pairs ($r < -0.7$, $p < 0.05$) were selected for further construction of ceRNA network. The circRNAs or lncRNAs could reduce the expression level of miRNAs through the ceRNA sponge mechanism.^{37,38} The circRNAs and lncRNAs targeting the selected DEmiRNAs were predicted by

ENCORI (<https://starbase.sysu.edu.cn/>).³⁹ At last, the ceRNA network of lncRNA/circRNA-DEmiRNA-OMDEG axis was constructed combining the significant DEmiRNA-OMDEG pairs and predicted circRNA/lncRNA-DEmiRNA pairs, and results were visualized by Cytoscape software (V.3.9.0).

2.7 | Potential link between metabolic disorder and immunity abnormality

The CIBERSORT algorithm (<https://cibersortx.stanford.edu/>) was used to analyze the normalized expression data of mRNAs to obtain the proportions of 22 kinds of immune cells in OLF tissues and normal LF tissues.⁴⁰ The immune cells not detected in OLF tissues and normal LF tissues were excluded for further analysis. The different proportion of immune cells between OLF tissues and normal LF tissues was compared by independent-samples *t* test, and the immune cells with $p < 0.05$ were considered as OLF-related infiltrating immune cells (OIICs). The correlation analysis between 10 hub OMDEGs and OIICs was performed using the Pearson test. To construct the regulatory network of DEmiRNA-OMDEG-OIIC axis, the significant hub OMDEG-OIIC pairs ($|r| > 0.70$, $p < 0.05$) were selected for the further intersection with significant DEmiRNA-OMDEG pairs ($r < -0.70$, $p < 0.05$).

2.8 | Cell culture and osteogenic differentiation

Cell culture was conducted in accordance with the protocol as described in our previous study.⁸ Briefly, the collected LF samples were minced into around 0.5 mm^3 pieces, and digested with 250 U/mL type I collagenase (Sigma-Aldrich, USA) at 37°C for 6 h. The specimen was cultured in Dulbecco's Modified Eagle's medium (Gibco, USA) containing 10% foetal bovine serum (Gibco, USA), 100 U/mL penicillin and 100 $\mu\text{g}/\text{mL}$ streptomycin at 37°C with 5% CO_2 . Cells from the two to third passages were used for the further cell experiments.

To check the osteogenic capacity of LF cells, LF cells were seeded in 6-well plates at a density of 1×10^5 per well and cultured in osteogenic medium (Procell, China). The alkaline phosphatase (ALP) activity was evaluated using the Alkaline Phosphatase Assay Kit (Beyotime, China). The Alizarin Red S (ARS) staining was used to assess the osteogenic capacity of LF cells following the instructions (Beyotime, China). To explore the effects of immune abnormality on the osteogenic differentiation of LF cells, we used the recombinant protein TNF- α (100 ng/mL) (PeproTech Inc, USA) to treat the LF cells.

2.9 | Quantitative real-time polymerase chain reaction (qRT-PCR)

Total RNA was extracted with the SteadyPure Universal RNA Extraction Kit (Accurate Biology, China). Reverse transcription and qRT-PCR were performed using Evo M-MLV RT Mix Kit (Accurate Biology,

China) and SYBR Green Premix Pro Taq HS qPCR Kit (Accurate Biology, China). GAPDH was applied as the internal control, and the expression of validated genes was calculated by the $2^{-\Delta\Delta Ct}$ method. The following primers were used in the qRT-PCR:

GAPDH-forward: 5'- CAGGAGGCATTGCTGATGAT-3';
 GAPDH-reverse: 5'- GAAGGCTGGGGCTCATT-3';
 GBE1-forward: 5'-ACTCATTACGCATGGGCTTGGTG-3';
 GBE1-reverse: 5'-CCGCTGGCATAATGGTAACTCTC-3';
 COL1A1-forward: 5'-AAAGATGGACTCAACGGTCTC-3';
 COL1A1-reverse: 5'- CATCGTGAGCCTTCTCTTGAG-3'.

2.10 | Small interfering RNA (siRNA) and transfection

The siRNA targeting the GBE1 (Sangon Biotech, China) was used to knock down the expression level of GBE1 in LF cells. The sequences for GBE1 siRNA were as follows:

Sense: 5'-CCACGGAGUCUAAGAAUUUUAUTT-3'; Antisense: 5'-AUAAAUUUUUAGACUCCGUGGTT-3'. The transfection of siRNA targeting GBE1 was conducted using the Lipofectamine 3000 Transfection Reagent (Invitrogen, USA) following the operation manual, and the transfection efficiency was tested by the qRT-PCR.

2.11 | Protein extraction and Western blot

The LF cells were washed with cold PBS three times and then treated with RIPA buffer (Solarbio, China). The concentration of protein was measured with the BCA Protein Assay Kit (Solarbio, China). Then, equal amounts of protein from each sample were separated by electrophoresis and then transferred onto PVDF membranes (Millipore, USA). The PVDF membranes were blocked in TBST containing 5% non-fat milk (Solarbio, China) for 2 h at room temperature. After blocking, the membranes were incubated with primary antibodies against COL1A1 (Abcam, USA) and GAPDH (Solarbio, China) for 2 hours, and then incubated with horseradish peroxidase-conjugated secondary antibody (Solarbio, China) for 1 hour at room temperature. The antibody binding was detected using the iBright CL1500 imaging system (Invitrogen, USA) after adding the ECL Western Blotting Substrate (Solarbio, China). The results of Western blot were analyzed using the iBright analysis software (Invitrogen, USA).

2.12 | Statistical analysis

The statistical analysis and result visualization were conducted by R 3.6.3 and GraphPad Prism 8.0 (San Diego, CA). The continuous variables between two groups, including the differences of metabolism score, proportion of immune cells, and the qRT-PCR or Western blot for candidate genes, were analyzed by the independent-samples *t*-test. All cell experiments were repeated at least three times

independently. Correlation analysis was performed by Pearson test, and results with $|r| > 0.70$ and $p < 0.05$ were considered statistically significant. The $p < 0.05$ indicated the results were significant.

3 | RESULTS

3.1 | Different metabolism status between OLF tissues and normal LF tissues

The metabolism score based on the metabolism-related gene list was calculated by the ssGSEA algorithm, and there was a significant difference between OLF tissues and normal LF tissues in terms of metabolism score ($p < 0.05$) (Figure 2A). Moreover, the two-dimensional PCA showed that the expression of metabolism-related genes could clearly distinguish the OLF tissues and normal LF tissues (Figure 2B). All these results indicated that metabolic disorder might be involved in the pathogenesis of OLF.

3.2 | Identification of OMDEGs between OLF tissues and normal LF tissues

As showed in the volcano plot, a total of 795 OLF-related differentially expressed genes (DEGs) (350 downregulated and 445 upregulated) were screened out based on the preset criterion of adjusted $p < 0.05$ and fold change > 2 (Figure 2C), and the heat map showed these genes could clearly distinguish OLF tissues and normal LF tissues (Figure 2D). Then, the intersection analysis between 795 OLF-related DEGs and 1383 metabolism-related genes was performed, and 49 OMDEGs were finally obtained (Figure 2E). The heat map showed 49 OMDEGs could clearly differentiate the OLF tissues from normal LF tissues (Figure 2F). The details of 49 OMDEGs were listed in Table 1, and 21 of them were up-regulated and 28 of them were down-regulated.

3.3 | Function enrichment analysis of OMDEGs

Gene ontology (GO) enrichment analysis of 49 OMDEGs, including biological process, cellular component, and molecular function, was performed using the DAVID database. OMDEGs were enriched in biological process of Lipid catabolic process, Triglyceride biosynthetic process, Gluconeogenesis, Cellular response to tumor necrosis factor, and so on (Figure 3A). With respect to cellular component, these OMDEGs were mainly enriched in Endoplasmic reticulum membrane, Golgi membrane, Endoplasmic reticulum, Mitochondrion, Phosphatidylinositol 3-kinase complex, and so on (Figure 3B). The molecular function showed these OMDEGs were mainly enriched in Hyaluronan synthase activity, Oxysterol binding, Kinase activity, and Phosphatidylinositol-4-phosphate binding (Figure 3C). With respect to the KEGG pathway, these 49 OMDEGs mainly participated in the Insulin resistance, Metabolic pathways, AMPK signaling pathway, Insulin signaling

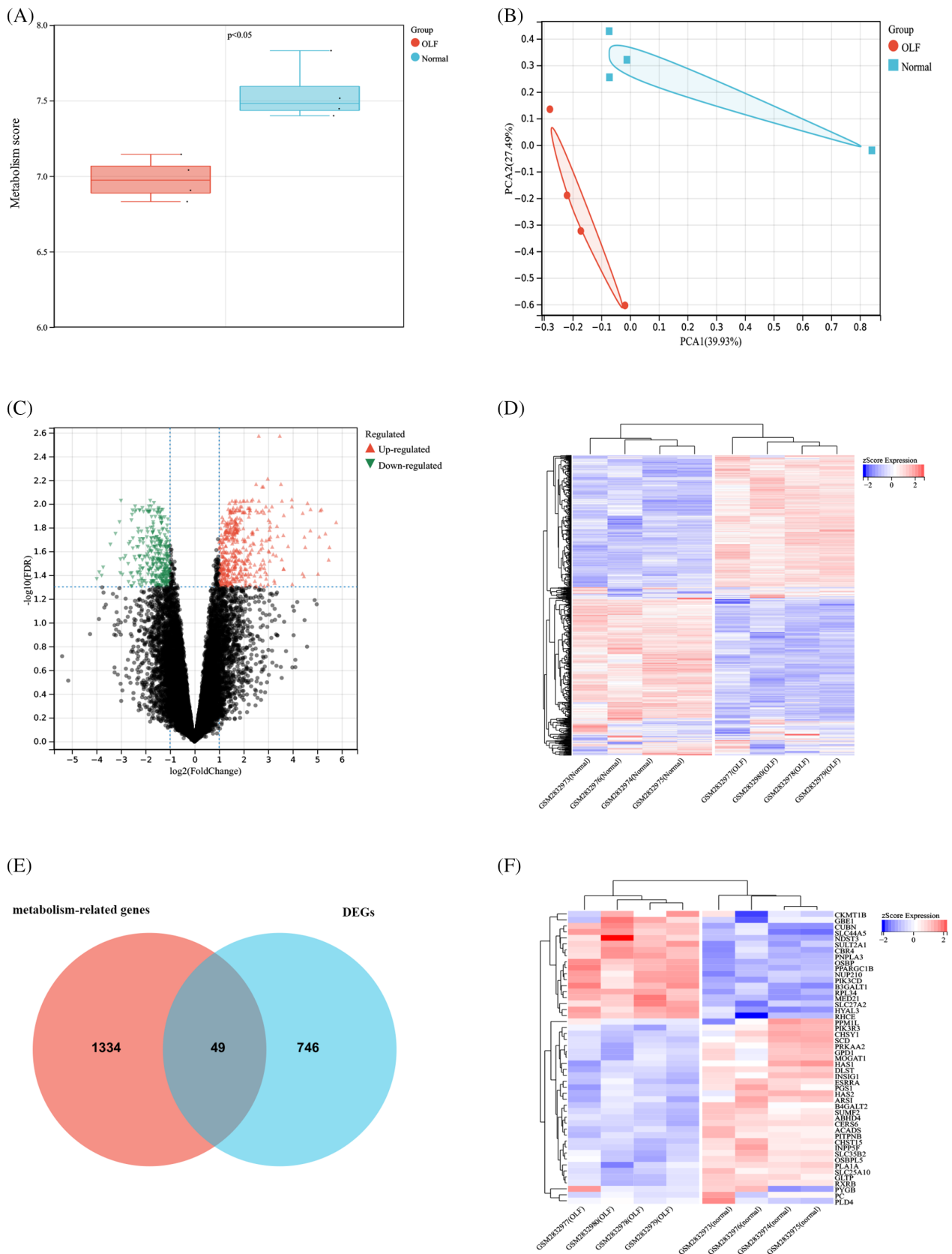


FIGURE 2 Metabolic disorder might play important roles in the development of OLF. (A) Comparison of metabolism score between OLF tissues and normal LF tissues; (B) PCA of metabolism-related genes; (C) Volcano plot of DEGs; (D) Heat map of DEGs; (E) Venn diagram to obtain the OMDEGs; (F) Heat map of OMDEGs.

TABLE 1 The details of 49 OMDEGs.

Expression	Gene symbols	Number (n)
Up-regulated	RPL34, B3GALT1, GBE1, HYAL3, NDST3, NUP210, PC, RHCE, CBR4, CERS6, CUBN, MED21, OSBP, PIK3CD, PLD4, PNPLA3, PPARGC1B, PPM1L, SLC27A2, SLC44A5, SULT2A1	21
Down-regulated	CKMT1B, DLST, SLC25A10, B4GALT2, CHST15, CHSY1, HAS1, HAS2, PYGB, SLC35B2, ABHD4, ACADS, ARSI, ESRRA, GLTP, GPD1, INPP5F, INSIG1, MOGAT1, OSBPL5, PGS1, PIK3R3, PITPNB, PLA1A, PRKAA2, RXRB, SCD, SUMF2	28

Abbreviation: OMDEGs, OLF-related and metabolism-related differentially expressed genes.

pathway, mTOR signaling pathway, and PPAR signaling pathway (Figure 3D).

3.4 | PPI network analysis of OMDEGs

PPI network containing 49 nodes and 30 edges was constructed using the STRING online database, and the interaction pairs with interaction score >0.40 were selected for further visualization using Cytoscape software (Figure 3E). Ten hub OMDEGs were selected ranked by the Degree in the cytoHubba analysis, including SCD, OSBP, PNPLA3, MOGAT1, PC, CHSY1, SLC27A2, PIK3R3, GPD1, and GBE1 (Figure 3F), and details of these 10 hub OMDEGs were listed in Table 2. The correlation analysis among 10 hub OMDEGs was also performed, and 31 significantly correlated pairs were obtained, for instance, SCD was most positively associated with CHSY1 ($r = 0.97$, $p < 0.05$) and negatively associated with PNPLA3 ($r = -0.86$, $p < 0.05$) (Figure 3G).

3.5 | Construction of ceRNA network based on miRNA-mRNA pairs

A total of 186 targeted miRNAs for 10 hub OMDEGs were predicted using the TargetScan 7.2 (Table S2). Fifty-one differentially expressed miRNAs (DEmiRNAs) were obtained according to the criteria of $p < 0.05$ and fold change >2 (Figure 4A), and heat map showed these 51 DEmiRNAs could clearly distinguish the OLF tissues and normal LF tissues (Figure 4B). Subsequently, 11 candidate miRNAs were acquired by the intersection analysis of DEmiRNAs with predicted miRNAs (hsa-miR-382-5p, hsa-miR-181a-5p, hsa-miR-181b-5p, hsa-miR-495-3p, hsa-miR-381-3p, hsa-miR-134-5p, hsa-miR-375, hsa-miR-19b-3p, hsa-miR-23b-3p, hsa-miR-32-5p, hsa-miR-144-3p). Then, the correlation analysis between 10 hub OMDEGs and 11 candidate miRNAs were performed, and only miRNA-mRNA pairs with $r < -0.7$ and $p < 0.05$ were selected for the construction of ceRNA

network (Figure S1). Finally, 8 miRNA-mRNA pairs containing 5 DEmiRNAs (hsa-miR-181b-5p, hsa-miR-181a-5p, hsa-miR-23b-3p, hsa-miR-375, hsa-miR-381-3p) and 3 hub OMDEGs (SCD, OSBP, PIK3R3) were remained (Figure 4C). The targeted circRNAs and lncRNAs for these five remained DEmiRNAs were predicted using the ENCORI database (Table S3), and the ceRNA network of circRNA-DEmiRNA-OMDEG (Figure 4D) and lncRNA-DEmiRNA-OMDEG (Figure 4E) were constructed, respectively.

3.6 | Potential link between metabolic disorder and immunity abnormality

The details of infiltrating immune cells in 4 OLF tissues and 4 normal LF tissues were shown in Figure 5A, and the violin plot presented there was a significant difference between OLF tissues and normal LF tissues in terms of resting memory CD4+ T cells ($p < 0.05$), gamma delta T cells ($p < 0.05$), M2 macrophages ($p < 0.05$), and resting mast cells ($p < 0.05$) (Figure 5B), and these 4 infiltrating immune cells were considered as OIICs. Then, the correlation analysis between 10 hub OMDEGs and 4 OLF-related infiltrating immune cells (OIICs) was performed, and 20 significantly related OMDEG-OIIC pairs were obtained with the criteria of $|r| > 0.70$ and $p < 0.05$ (Figure 5C), such as the association of SCD with resting mast cells ($r = -0.84$, $p < 0.01$) (Figure 5D), resting memory CD4+ T cells ($r = 0.79$, $p = 0.02$) (Figure 5E), and gamma delta T cells ($r = -0.76$, $p = 0.03$) (Figure 5F). To further elucidate the potential link between metabolic disorder and immunity abnormality in OLF, a DEmiRNA-OMDEG-OIIC regulatory network was built (Figure 6).

3.7 | Cell experiment validation

The ossified LF tissues compressed the spinal cord and lead to the thoracic myelopathy (Figure 7A). The LF cells were homogeneous and typical fibrocyte shape (Figure 7B). To validate the key roles of OMDEGs, we randomly selected the GBE1, one of the 10 hub OMDEGs, for the further validation. Similar to the chip sequencing data, the expression level of GBE1 was obviously increased in the OLF tissues compared with normal LF tissues (Figure 7C). Moreover, the efficiency of GBE1 siRNA was examined, and the expression level of GBE1 was distinctly decreased (Figure 7D). The mRNA (Figure 7E) and protein (Figure 7F,G) level of osteogenesis-related gene (COL1A1) was significantly decreased when knocking down the GBE1 expression in LF cells. The ALP and ARS staining were both distinctly reduced when knocking down the GBE1 expression in LF cells under the osteogenic differentiation (Figure 7H). To validate the important role of immunity abnormality in the pathogenesis of OLF, the inflammatory factor TNF- α was used to stimulate the LF cells under the osteogenic induction, and the TNF- α significantly increase the mRNA (Figure 7I) and protein (Figure 7J,K) level of osteogenesis-related gene (COL1A1). Moreover, the ALP and ARS staining were both distinctly increased when adding the TNF- α to LF cells (Figure 7L).

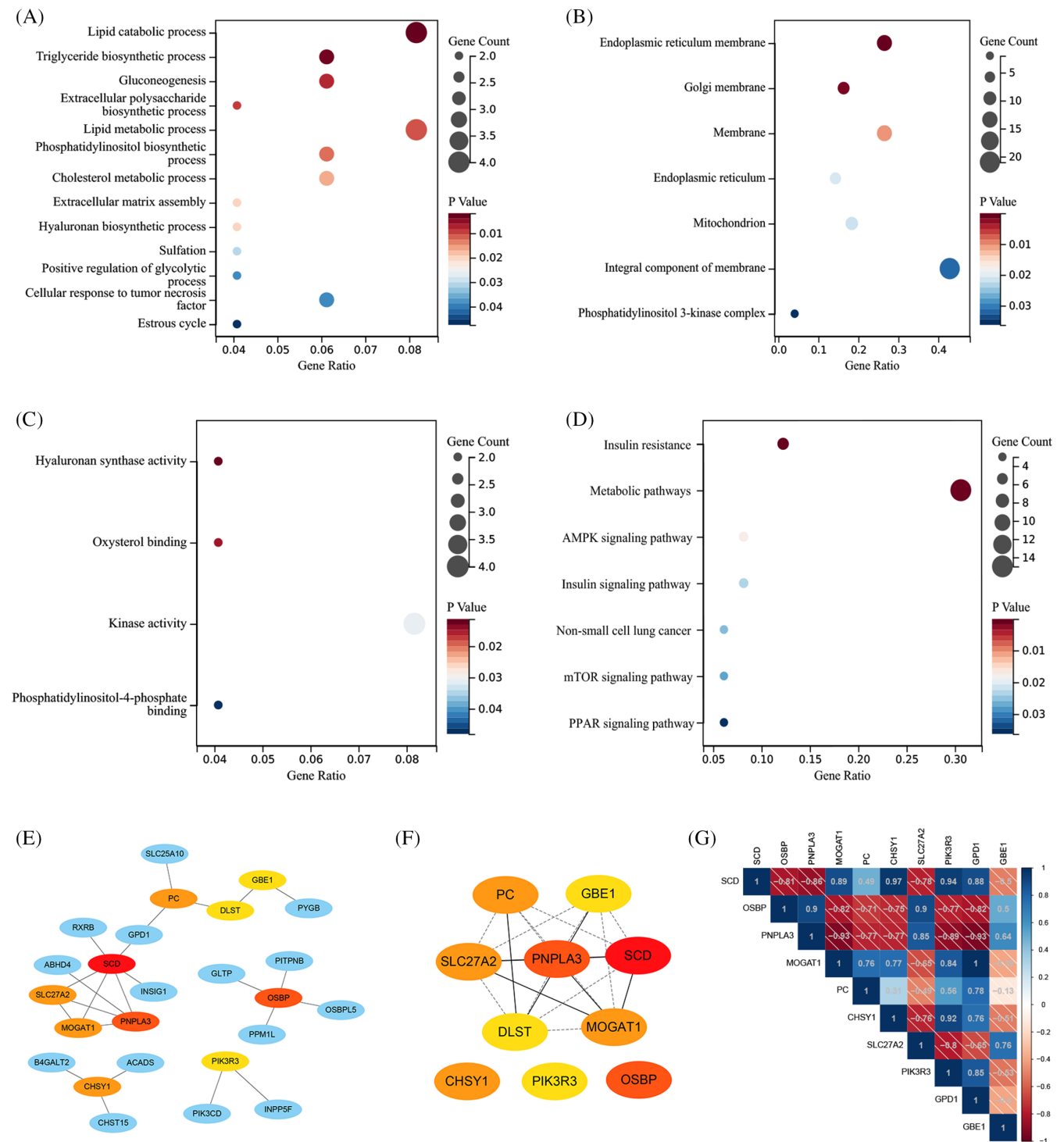


FIGURE 3 GO analysis, KEGG pathway, and PPI analysis of OMDEGs. (A) biological process in GO analysis; (B) cellular component in GO analysis; (C) molecular function in GO analysis; (D) KEGG pathway; (E) PPI analysis of OMDEGs; (F) Determination of 10 hub OMDEGs; (G) Correlation analysis among 10 hub OMDEGs.

4 | DISCUSSION

OLF is a characteristic heterotopic ossification disease, which can lead to the thoracic stenosis and induce the spinal cord injury.⁴¹ Although increasing researches have been conducted to determine the risk

factors and explore the etiology of OLF, the underlying mechanism of pathogenesis remains obscure up to now. Previous studies have indicated that the population with obesity or diabetes were more likely to suffer from the OLF, which indicated that metabolic disorder might play important roles in the pathogenesis of OLF.^{3,10,14,18} Some

TABLE 2 The details of top 10 hub OMDEGs.

Gene symbols	Full names	Gene function	Log2 (fold change)	p value	Regulation
SCD	Stearoyl-CoA desaturase	This gene encodes an enzyme involved in fatty acid biosynthesis, primarily the synthesis of oleic acid.	-1.1658151	0.02777	Down
OSBP	Oxysterol binding protein	This gene is an intracellular protein that is believed to transport sterols from lysosomes to the nucleus.	1.248215	0.01713	Up
PNPLA3	Patatin like phospholipase domain containing 3	This gene is a triacylglycerol lipase that mediates triacylglycerol hydrolysis in adipocytes.	1.6007371	0.02574	Up
MOGAT1	Monoacylglycerol O-acyltransferase 1	This gene catalyzes the synthesis of diacylglycerols, the precursor of physiologically important lipids such as triacylglycerol and phospholipids.	-1.4651819	0.04955	Down
PC	Pyruvate carboxylase	This gene encodes pyruvate carboxylase, which requires biotin and ATP to catalyze the carboxylation of pyruvate to oxaloacetate.	2.2686795	0.02227	Up
CHSY1	Chondroitin sulfate synthase 1	This gene encodes a member of the chondroitin N-acetylgalactosaminyltransferase family, which play critical roles in the biosynthesis of chondroitin sulfate.	-1.4798438	0.03555	Down
SLC27A2	Solute carrier family 27 member 2	The protein encoded by this gene is an isozyme of long-chain fatty-acid-coenzyme A ligase family.	2.040629	0.03143	Up
PIK3R3	Phosphoinositide-3-kinase regulatory subunit 3	The protein encoded by this gene represents a regulatory subunit of PI3K and contains two SH2 domains through which it binds activated protein tyrosine kinases to regulate their activity.	-2.1174822	0.03514	Down
GPD1	Glycerol-3-phosphate dehydrogenase 1	The encoded protein by this gene plays a critical role in carbohydrate and lipid metabolism by catalyzing the reversible conversion of dihydroxyacetone phosphate (DHAP) and reduced nicotinic adenine dinucleotide (NADH) to glycerol-3-phosphate (G3P) and NAD ⁺ .	-3.7888723	0.04021	Down
GBE1	1,4-alpha-glucan branching enzyme 1	The protein encoded by this gene is a glycogen branching enzyme that catalyzes the transfer of alpha-1,4-linked glucosyl units from the outer end of a glycogen chain to an alpha-1,6 position on the same or a neighboring glycogen chain.	1.6410789	0.01604	Up

Abbreviation: OMDEGs, OLF-related and metabolism-related differentially expressed genes.

bioinformatic analyses were conducted to investigate the role of ceRNA network or immunity abnormality in the onset and development of OLF,^{31,42} however, no study was especially conducted to determine the role of metabolic disorder in the pathogenesis of OLF with strict bioinformatic algorithms. In the current study, we firstly observed the difference of metabolism score between OLF tissues and normal LF tissues, which presented that metabolic disorder might be an important etiological factor for OLF. Then, to further explore the role of metabolic disorder in the pathogenesis of OLF, we screened out 49 OMDEGs, determined their key biological functions, selected 10 hub OMDEGs, constructed the relevant ceRNA network, and explored the potential link between metabolic disorder and immunity abnormality in the development of OLF.

In this study, we found there was a significant relationship between the metabolic disorder and OLF using the ssGSEA algorithm and PCA. Few but some studies have been conducted to explore the underlying mechanism of metabolic disorder in the pathogenesis of ossification of the spinal ligaments.^{10,43,44} Li et al. study showed that hyperinsulinemia could stimulate the BMP-2-induced osteogenic differentiation of spinal ligament cells via the activation of insulin receptor and PI3K/Akt pathway and the suppression of ERK.⁴³ Fan et al.

reported that leptin could promote the osteogenesis of thoracic OLF via the activation of signaling molecules STAT3, Runx2, and SRC-1.¹⁰ In our study, we screened out 49 OMDEGs, the function analysis of KEGG pathways showed these genes might participate the osteogenesis through the following pathways: insulin resistance, AMPK signaling pathway, insulin signaling pathway, mTOR signaling pathway, and PPAR signaling pathway. In fact, several studies have observed the vital role of these biological pathways in the osteogenesis process.⁴⁵⁻⁴⁷ Chen et al. found that adiponectin could accelerate the osteogenic differentiation of adipose-derived mesenchymal stem cells (MSCs) through the activation of APPL1-AMPK signaling.⁴⁵ Cui et al. study indicated the osteogenic differentiation of bone marrow MSCs could be improved through the PI3K/AKT/mTOR signaling pathway.⁴⁶ Wang et al. study presented there was a reduction of PPAR signaling pathway on the aligned fibers, which might promote the osteogenesis.⁴⁷ However, no research has been conducted to explore the role of these pathways in the development of OLF, which might be a promising research direction in the future.

Ten hub OMDEGs were screened out based on the PPI analysis in this study, but only 1 of 10 hub OMDEGs, named SCD, was reported to be engaged in the osteogenic differentiation of adipose-

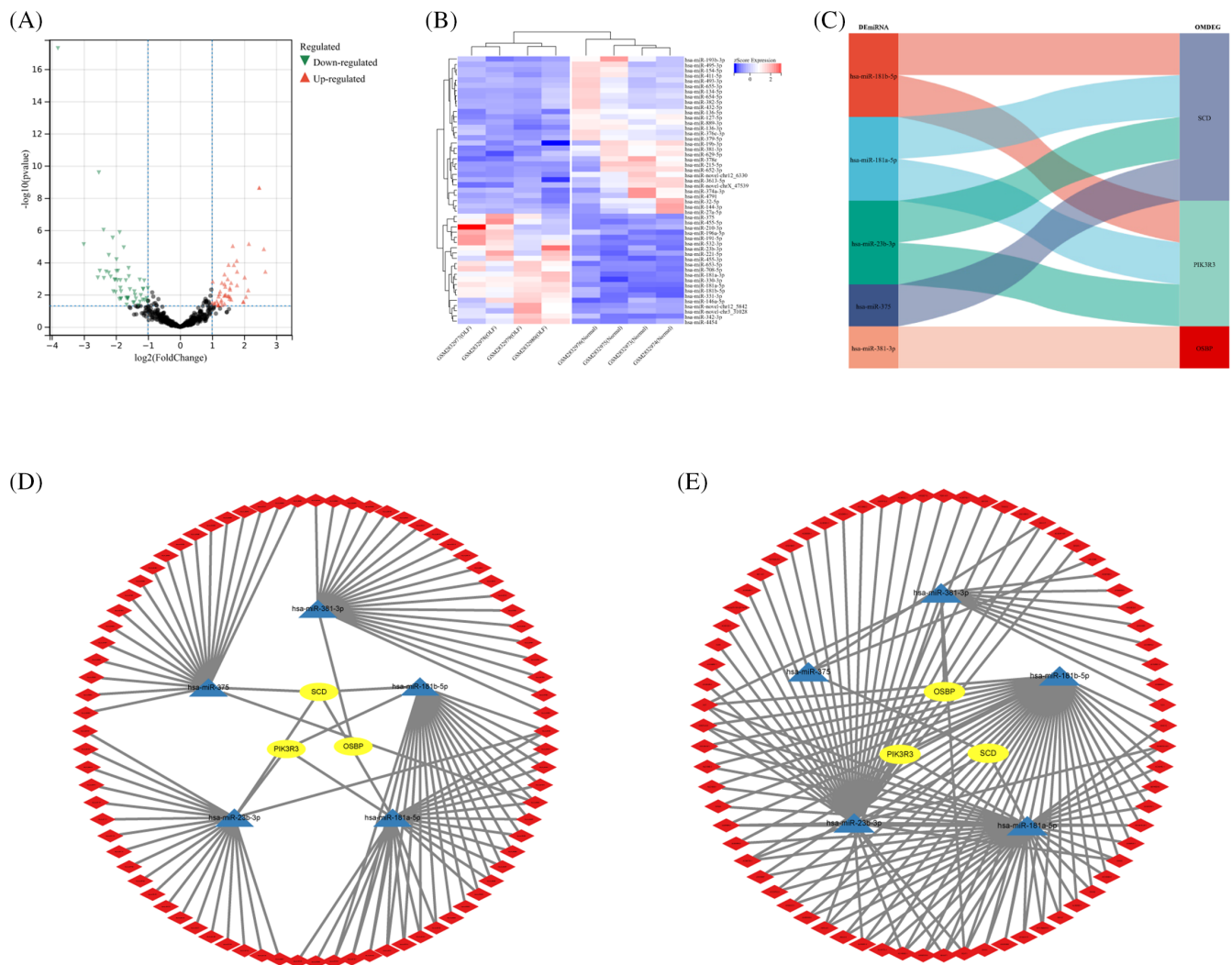


FIGURE 4 Construction of circRNA/lncRNA-DEmiRNA-OMDEG network. (A) Volcano plot of DEmiRNAs; (B) Heat map of DEmiRNAs; (C) Significant DEmiRNA-OMDEG pairs; (D) CircRNA-DEmiRNA-OMDEG network; (E) LncRNA-DEmiRNA-OMDEG network.

derived MSCs.⁴⁸ The authors reported that Let-7c regulated the adipose-derived MSCs under oxidative stress by targeting SCD to activate the Wnt/ β -catenin signaling. But the metabolic role of SCD in the osteogenic differentiation of MSCs were not investigated in their study.⁴⁸ To our knowledge, there was no report about the osteogenic roles of the other 9 hub OMDEGs up to now, which needed our special attention in future work. Moreover, to further explore the potential underlying mechanism of these 10 hub OMDEGs, we built the ceRNA network based on 8 miRNA-mRNA pairs. It was very likely that metabolic disorder contributed to the development of OLF through these ceRNA networks of circRNA/lncRNA-DEmiRNA-OMDEG axis, which were firstly suggested to be further explored. Moreover, we randomly selected the GBE1, one of 10 hub OMDEGs, to explore its role in the osteogenesis of LF, and our findings showed that the reduction of GBE1 expression in LF cells could significantly decrease the osteogenic potential of LF cells. However, the metabolic roles of hub OMDEGs in the osteogenic differentiation of LF cells

have not been investigated, which should be given special attention in the future.

Accumulated evidence manifested there was a crucial relationship between metabolic disorder and immunity abnormality in the development of diseases.¹³ Besides, previous studies indicated that inflammation might promote the onset and progression of OLF.^{31,49} In this study, to verify the important role of immunity abnormality in the OLF, we used the recombinant TNF- α to treat the LF cells, and we discovered that the addition of TNF- α obviously increased the osteogenic differentiation of LF cells. We found there was a significantly different percentage of immune cells between OLF tissues and normal LF tissues in terms of resting memory CD4+ T cells, gamma delta T cells, M2 macrophages, and resting mast cells, which indicated that immunity abnormality might be associated with the OLF. For instance, M2 macrophages were famous anti-inflammatory cells, and could partly antagonize the pro-inflammatory function of M1 macrophages, therefore, the relatively lower percentage of M2 macrophages in OLF

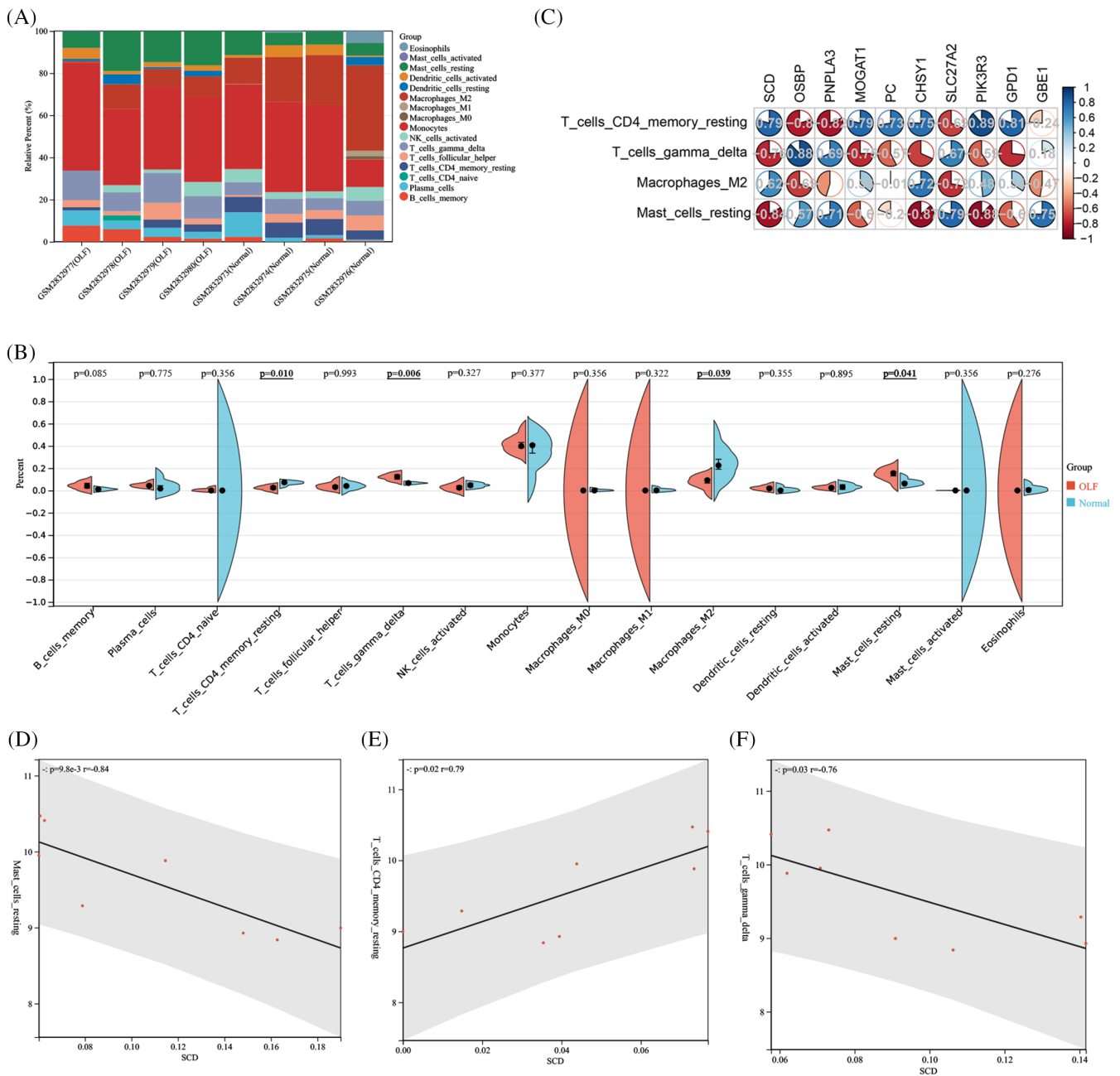


FIGURE 5 Potential link between metabolic disorder and immunity abnormality in the development of OLF. (A) Immune cells in OLF tissues and normal LF tissues; (B) Violin plot of immune cells; (C) Correlation analysis hub OMDEGs and between OIICs; (D) Correlation analysis between SCD and Mast_cells_resting; (E) Correlation analysis between SCD and T_cells_CD4_memory_resting; (F) Correlation analysis between SCD and T_cells_gamma_delta.

tissues might aggravate the local inflammation and contribute to the OLF. To further explore whether the metabolic disorder potentially induced the OLF via regulating the immune status, the correlation analysis between hub OMDEGs and OIICs was performed, and several significant correlated OMDEG-OIIC pairs were observed, such as SCD and resting memory CD4+ T cells. Future studies should be carried out to determine the relevant role of these OIICs in the OLF, especially resting memory CD4+ T cells, which were significantly

related to most of 10 hub OMDEGs. More importantly, it should be noted, despite the unclear underlying mechanism, the OMDEGs might participate in the OLF through the regulation of immune status. To further investigate the potential mechanism, we constructed the DE miRNA-OMDEG-OIIC regulatory network, which was very worth of further study.

Several limitations should be considered when interpreting our results. First, this bioinformatic analysis was conducted based on the

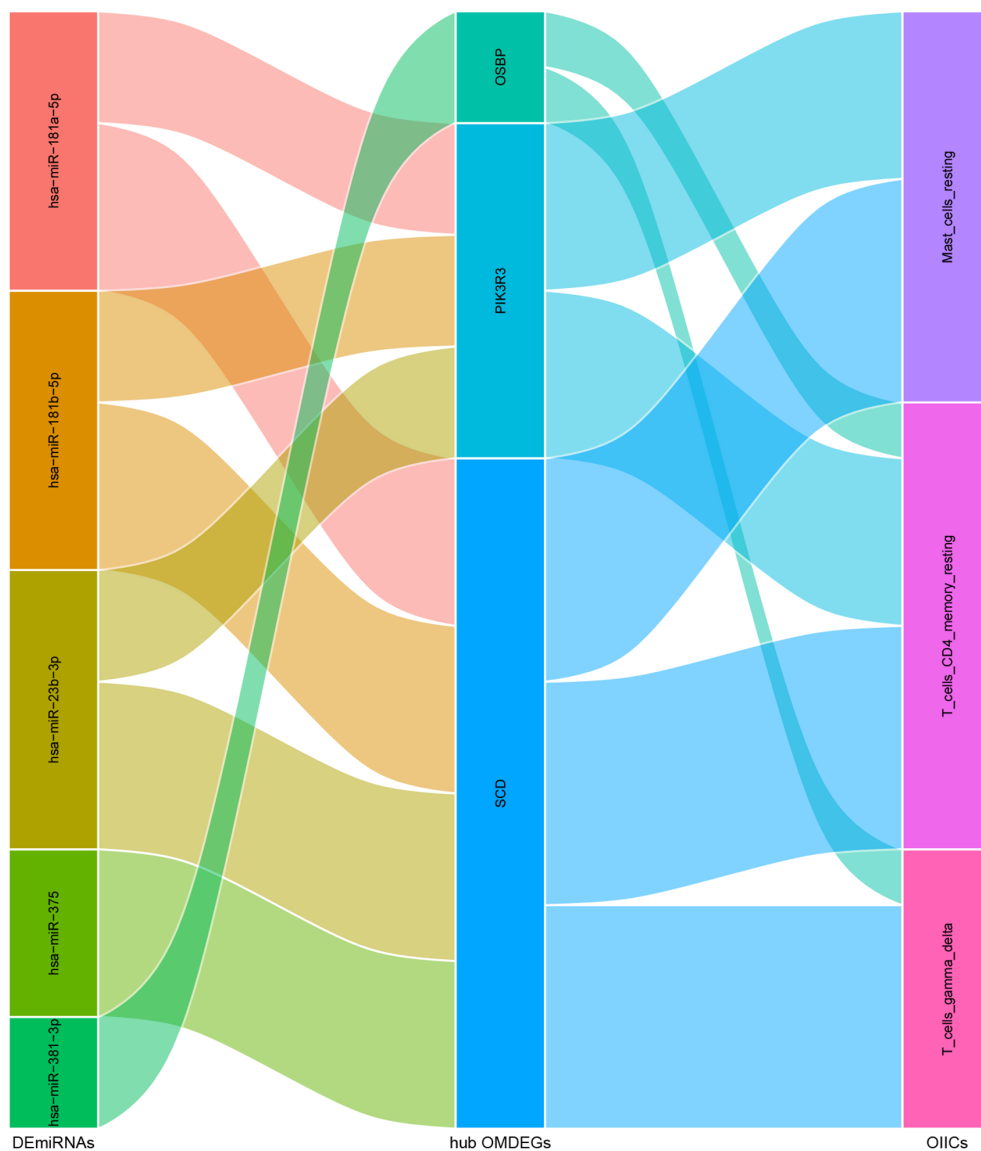


FIGURE 6 Construction of DEmiRNA-OMDEG-OIIC regulatory network.

sequencing data from 4 OLF subjects and 4 non-OLF subjects, which was a relatively small sample size and hindered the further analysis. However, there was no other sequencing data relevant to the OLF in public database, which might be attributed to the rarity of this disease. Second, all the analyses in this study were conducted using the bioinformatic methodologies and some bits of cell experiments, further animal experiments should be conducted to validate our findings in the future. Third, the change of metabolism-related genes could not be completely identified with metabolic disorders, but there was a correlation between them to some extent, which might provide new insights about the metabolic disorder in OLF. Despite these limitations, for the first time, we preliminarily verified the vital role of metabolic disorder in the pathogenesis of OLF, screened out several important OMDEGs, constructed the ceRNA network, and discovered the potential link between metabolic disturbance and immune abnormality in OLF via analyzing the metabolism-related genes, which provided new insights into the pathogenesis and promising therapeutic

targets of OLF, and had the potential to elucidate the higher prevalence of OLF in obese population.

5 | CONCLUSIONS

Taken together, through strict bioinformatic approaches based on whole transcriptomic data of OLF and cell experiments, in this study, we demonstrated metabolic disorder played important roles in the pathogenesis of OLF. We selected 10 hub OMDEGs (e.g., SCD, OSBP, PNPLA3, and MOGAT1) deserving deeper investigation, and constructed the circRNA/lncRNA-DEmiRNA-OMDEG network deserving further validation. Moreover, we discovered the potential link between metabolic disorder and immune abnormality in the development of OLF. Therefore, our study suggested that the metabolic disorder might promote the development of OLF via the specific ceRNA networks and change of immune status in LF tissues.

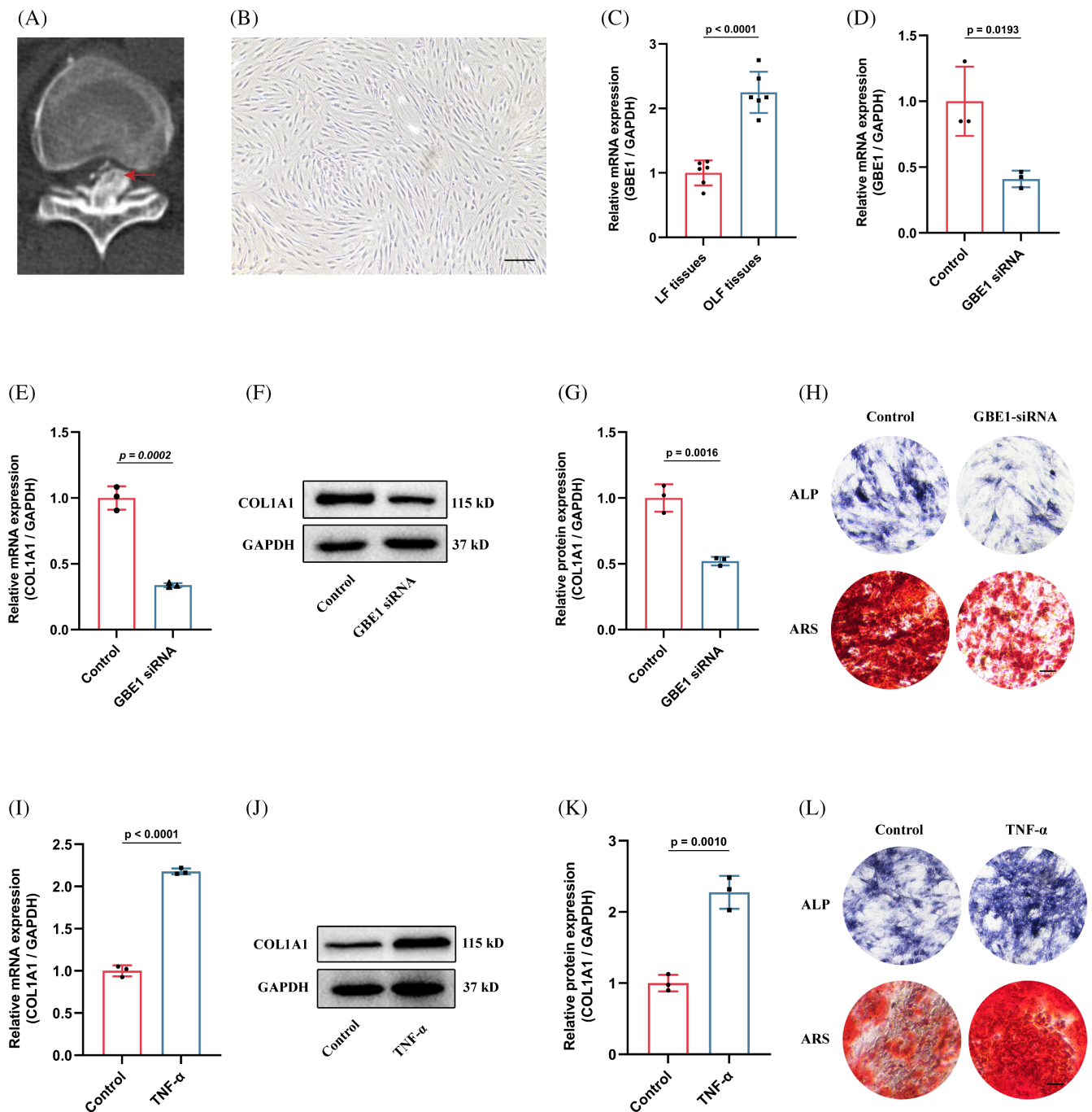


FIGURE 7 Experiment validation. (A) Ossified LF tissues in thoracic computed tomography; (B) LF cells extracted from LF tissues (scale bar: 50 μ m); (C) GBE1 was significantly increased in OLF tissues compared with normal LF tissues; (D) GBE1 was obviously decreased when transfecting the LF cells with the siRNA targeting GBE1; (E–G) The mRNA (E) and protein (F,G) level of COL1A1 was significantly decreased when knocking down the GBE1 expression; (H) ALP and ARS staining were both distinctly reduced when knocking down the GBE1 expression (scale bar: 25 μ m); (I–K) The mRNA (I) and protein (J, K) level of COL1A1 was significantly increased when adding TNF- α to LF cells; (L) ALP and ARS staining were both distinctly increased when adding TNF- α to LF cells (scale bar: 25 μ m).

AUTHOR CONTRIBUTIONS

LW designed the research study. ZYZ and JS performed the research. XQ and LJL provided help and advice. ZYZ and XQ analyzed the data. ZYZ and JS wrote the manuscript. All authors contributed to editorial changes in the manuscript. All authors read and approved the final

manuscript. Yongzhao Zhao, Qian Xiang and Shuai Jiang contributed equally to this research, and were listed as the co-first authors.

ACKNOWLEDGMENTS

The authors have nothing to report.

FUNDING INFORMATION

This work was supported by the National Natural Science Foundation of China (Grant No. 82172480).

CONFLICT OF INTEREST STATEMENT

The authors declare no conflicts of interest.

DATA AVAILABILITY STATEMENT

The original contributions presented in the study are included in the article/supplementary material; further inquiries can be directed to the corresponding author/s.

REFERENCES

- Aizawa T, Sato T, Sasaki H, Kusakabe T, Morozumi N, Kokubun S. Thoracic myelopathy caused by ossification of the ligamentum flavum: clinical features and surgical results in the Japanese population. *J Neurosurg Spine*. 2006;5(6):514-519.
- Guo JJ, Luk KD, Karppinen J, Yang H, Cheung KM. Prevalence, distribution, and morphology of ossification of the ligamentum flavum: a population study of one thousand seven hundred thirty-six magnetic resonance imaging scans. *Spine*. 2010;35(1):51-56.
- Lang N, Yuan HS, Wang HL, et al. Epidemiological survey of ossification of the ligamentum flavum in thoracic spine: CT imaging observation of 993 cases. *Eur Spine J*. 2013;22(4):857-862.
- Aizawa T, Sato T, Sasaki H, et al. Results of surgical treatment for thoracic myelopathy: minimum 2-year follow-up study in 132 patients. *J Neurosurg Spine*. 2007;7(1):13-20.
- Yamada T, Shindo S, Yoshii T, et al. Surgical outcomes of the thoracic ossification of ligamentum flavum: a retrospective analysis of 61 cases. *BMC Musculoskelet Disord*. 2021;22(1):7.
- Baba S, Shiboi R, Yokosuka J, et al. Microendoscopic posterior decompression for treating thoracic myelopathy caused by ossification of the Ligamentum Flavum: case series. *Medicina (Kaunas)*. 2020;56(12):684.
- Kong Q, Ma X, Li F, et al. COL6A1 polymorphisms associated with ossification of the ligamentum flavum and ossification of the posterior longitudinal ligament. *Spine*. 2007;32(25):2834-2838.
- Yang J, Chen G, Fan T, Qu X. M1 macrophage-derived oncostatin M induces osteogenic differentiation of ligamentum flavum cells through the JAK2/STAT3 pathway. *JOR Spine*. 2024;7(1):e1290.
- Cai HX, Yayama T, Uchida K, et al. Cyclic tensile strain facilitates the ossification of ligamentum flavum through β -catenin signaling pathway: in vitro analysis. *Spine*. 2012;37(11):E639-E646.
- Fan D, Chen Z, Chen Y, Shang Y. Mechanistic roles of leptin in osteogenic stimulation in thoracic ligament flavum cells. *J Biol Chem*. 2007;282(41):29958-29966.
- Chakraborty S, Balan M, Sabarwal A, Choueiri TK, Pal S. Metabolic reprogramming in renal cancer: events of a metabolic disease. *Biochim Biophys Acta Rev Cancer*. 2021;1876(1):188559.
- Hameed I, Masoodi SR, Mir SA, Nabi M, Ghazanfar K, Ganai BA. Type 2 diabetes mellitus: from a metabolic disorder to an inflammatory condition. *World J Diabetes*. 2015;6(4):598-612.
- Saltiel AR, Olefsky JM. Inflammatory mechanisms linking obesity and metabolic disease. *J Clin Invest*. 2017;127(1):1-4.
- Endo T, Koike Y, Hisada Y, et al. Aggravation of ossified ligamentum flavum lesion is associated with the degree of obesity. *Global Spine J*. 2021;13:1325-1331. doi:10.1177/21925682211031514
- Chaput CD, Siddiqui M, Rahm MD. Obesity and calcification of the ligaments of the spine: a comprehensive CT analysis of the entire spine in a random trauma population. *Spine J*. 2019;19(8):1346-1353.
- Endo T, Takahata M, Koike Y, Iwasaki N. Clinical characteristics of patients with thoracic myelopathy caused by ossification of the posterior longitudinal ligament. *J Bone Miner Metab*. 2020;38(1):63-69.
- Kawaguchi Y, Yasuda T, Seki S, et al. Variables affecting postsurgical prognosis of thoracic myelopathy caused by ossification of the ligamentum flavum. *Spine J*. 2013;13(9):1095-1107.
- Kim SI, Ha KY, Lee JW, Kim YH. Prevalence and related clinical factors of thoracic ossification of the ligamentum flavum—a computed tomography-based cross-sectional study. *Spine J*. 2018;18(4):551-557.
- Zhang H, Wang C, Wang D, et al. Predictive risk factors of poor preliminary postoperative outcome for thoracic ossification of the Ligamentum Flavum. *Orthop Surg*. 2021;13(2):408-416.
- Shirakura Y, Sugiyama T, Tanaka H, Taguchi T, Kawai S. Hyperleptinemia in female patients with ossification of spinal ligaments. *Biochem Biophys Res Commun*. 2000;267(3):752-755.
- Zhao Y, Xiang Q, Lin J, Jiang S, Li W. High body mass index is associated with an increased risk of the onset and severity of ossification of spinal ligaments. *Front Surg*. 2022;9:941672.
- Zhao Y, Xiang Q, Lin J, Jiang S, Li W. High systemic immune-inflammation index and body mass index are independent risk factors of the thoracic ossification of the ligamentum flavum. *Mediators Inflamm*. 2022;2022:4300894.
- Xin X, Li Q, Fang J, Zhao T. LncRNA HOTAIR: a potential prognostic factor and therapeutic target in human cancers. *Front Oncol*. 2021;11:679244.
- Chen LL, Yang L. Regulation of circRNA biogenesis. *RNA Biol*. 2015;12(4):381-388.
- Qu S, Zhong Y, Shang R, et al. The emerging landscape of circular RNA in life processes. *RNA Biol*. 2017;14(8):992-999.
- Lee RC, Feinbaum RL, Ambros V. The *C. elegans* heterochronic gene *lin-4* encodes small RNAs with antisense complementarity to *lin-14*. *Cell*. 1993;75(5):843-854.
- Sakshi S, Jayasuriya R, Ganesan K, Xu B, Ramkumar KM. Role of circRNA-miRNA-mRNA interaction network in diabetes and its associated complications. *Mol Ther Nucleic Acids*. 2021;26:1291-1302.
- Kong H, Sun ML, Zhang XA, Wang XQ. Crosstalk among circRNA/lncRNA, miRNA, and mRNA in osteoarthritis. *Front Cell Dev Biol*. 2021;9:774370.
- Wang B, Chen Z, Meng X, Li M, Yang X, Zhang C. iTRAQ quantitative proteomic study in patients with thoracic ossification of the ligamentum flavum. *Biochem Biophys Res Commun*. 2017;487(4):834-839.
- Qu X, Xu G, Hou X, et al. M1 macrophage-derived Interleukin-6 promotes the osteogenic differentiation of Ligamentum Flavum cells. *Spine*. 2022;47(15):E527-e535.
- Zhang B, Chen G, Chen X, et al. Integrating Bioinformatic strategies with real-world data to infer distinctive Immunocyte infiltration landscape and immunologically relevant transcriptome fingerprints in ossification of Ligamentum Flavum. *J Inflamm Res*. 2021;14:3665-3685.
- Han Y, Hong Y, Li L, et al. A transcriptome-level study identifies changing expression profiles for ossification of the ligamentum flavum of the spine. *Mol Ther Nucleic Acids*. 2018;12:872-883.
- Subramanian A, Tamayo P, Mootha VK, et al. Gene set enrichment analysis: a knowledge-based approach for interpreting genome-wide expression profiles. *Proc Natl Acad Sci U S A*. 2005;102(43):15545-15550.
- Shannon P, Markiel A, Ozier O, et al. Cytoscape: a software environment for integrated models of biomolecular interaction networks. *Genome Res*. 2003;13(11):2498-2504.
- Agarwal V, Bell GW, Nam J-W, Bartel DP. Predicting effective microRNA target sites in mammalian mRNAs. *Elife*. 2015;4:e05005.
- Friedman RC, Farh KK, Burge CB, Bartel DP. Most mammalian mRNAs are conserved targets of microRNAs. *Genome Res*. 2009;19(1):92-105.
- Patop IL, Wüst S, Kadener S. Past, present, and future of circRNAs. *EMBO J*. 2019;38(16):e100836.
- Mattick JS, Amaral PP, Carninci P, et al. Long non-coding RNAs: definitions, functions, challenges and recommendations. *Nat Rev Mol Cell Biol*. 2023;24(6):430-447.

39. Li JH, Liu S, Zhou H, Qu LH, Yang JH. starBase v2.0: decoding miRNA-ceRNA, miRNA-ncRNA and protein-RNA interaction networks from large-scale CLIP-Seq data. *Nucleic Acids Res.* 2014;42:D92-D97.
40. Newman AM, Liu CL, Green MR, et al. Robust enumeration of cell subsets from tissue expression profiles. *Nat Methods.* 2015;12(5):453-457.
41. Hirabayashi S. Ossification of the ligamentum flavum. *Spine Surg Relat Res.* 2017;1(4):158-163.
42. Kong D, Zhao Q, Liu W, Wang F. Identification of crucial miRNAs and lncRNAs for ossification of ligamentum flavum. *Mol Med Rep.* 2019;20(2):1683-1699.
43. Li H, Liu D, Zhao CQ, Jiang LS, Dai LY. Insulin potentiates the proliferation and bone morphogenetic protein-2-induced osteogenic differentiation of rat spinal ligament cells via extracellular signal-regulated kinase and phosphatidylinositol 3-kinase. *Spine.* 2008;33(22):2394-2402.
44. Li H, Liu D, Zhao CQ, Jiang LS, Dai LY. High glucose promotes collagen synthesis by cultured cells from rat cervical posterior longitudinal ligament via transforming growth factor-beta1. *Eur Spine J.* 2008;17(6):873-881.
45. Chen T, Wu YW, Lu H, Guo Y, Tang ZH. Adiponectin enhances osteogenic differentiation in human adipose-derived stem cells by activating the APPL1-AMPK signaling pathway. *Biochem Biophys Res Commun.* 2015;461(2):237-242.
46. Cui H, Han G, Sun B, et al. Activating PIK3CA mutation promotes osteogenesis of bone marrow mesenchymal stem cells in macrodactyly. *Cell Death Dis.* 2020;11(7):505.
47. Wang Y, Gao R, Wang PP, et al. The differential effects of aligned electrospun PHBHHx fibers on adipogenic and osteogenic potential of MSCs through the regulation of PPAR γ signaling. *Biomaterials.* 2012;33(2):485-493.
48. Zhou Z, Lu Y, Wang Y, Du L, Zhang Y, Tao J. Let-7c regulates proliferation and osteodifferentiation of human adipose-derived mesenchymal stem cells under oxidative stress by targeting SCD-1. *Am J Physiol Cell Physiol.* 2019;316(1):C57-c69.
49. Zhang C, Chen Z, Meng X, Li M, Zhang L, Huang A. The involvement and possible mechanism of pro-inflammatory tumor necrosis factor alpha (TNF- α) in thoracic ossification of the ligamentum flavum. *PLoS One.* 2017;12(6):e0178986.

SUPPORTING INFORMATION

Additional supporting information can be found online in the Supporting Information section at the end of this article.

How to cite this article: Zhao Y, Xiang Q, Jiang S, Lin J, Li W. Revealing the novel metabolism-related genes in the ossification of the ligamentum flavum based on whole transcriptomic data. *JOR Spine.* 2024;7(3):e1357. doi:[10.1002/jsp2.1357](https://doi.org/10.1002/jsp2.1357)